Published in final edited form as:
Free Radic Biol Med. 2013 May ; 58: 126–133. doi:10.1016/j.freeradbiomed.2012.12.020.

Nitroarachidonic acid prevents NADPH oxidase assembly and superoxide radical production in activated macrophages

Lucía González-Perilli, **María Noel Álvarez**, **Carolina Prolo**, **Rafael Radi**, **Homero Rubbo**, and **Andrés Trostchansky**[*]
Departamento de Bioquímica and Center for Free Radical and Biomedical Research, Facultad de Medicina-Universidad de la República, Montevideo, Uruguay

Abstract

Nitration of arachidonic acid (AA) to nitroarachidonic acid ($AANO_2$) leads to anti-inflammatory intracellular activities during macrophage activation. However, less is known about the capacity of $AANO_2$ to regulate the production of reactive oxygen species (ROS) under pro-inflammatory conditions. One of the immediate responses upon macrophage activation involves the production of superoxide radical ($O_2^{\cdot-}$), due to the NADPH dependent univalent reduction of oxygen to $O_2^{\cdot-}$ by the phagocytic NADPH-oxidase isoform (NOX2), being the activity of NOX2 the main source of $O_2^{\cdot-}$ in monocytes/macrophages. Since NOX2 and AA pathways are connected, we propose that $AANO_2$can modulate macrophage activation by inhibiting $O_2^{\cdot-}$ formation by NOX2. When macrophages were activated in the presence of $AANO_2$, a significant inhibition of NOX2 activity was observed as evaluated by cytochrome c reduction, luminol chemiluminescence, Amplex Red fluorescence and flow cytometry; this process also occurs in physiological mimic conditions within the phagosomes. $AANO_2$ decreased $O_2^{\cdot-}$ production in a dose-(IC_{50}= 4.1 ± 1.8 μM $AANO_2$) and time-dependent manner. The observed inhibition was not due to a decreased phosphorylation of the cytosolic subunits (*e.g.* $p40^{phox}$ and $p47^{phox}$), as analyzed by immunoprecipitation and western blot. However, a reduction of the migration to the membrane of $p47^{phox}$ was obtained suggesting that the protective actions involve the prevention of the correct assembly of the active enzyme in the membrane. Finally, the observed *in vitro* effects were confirmed in an *in vivo* inflammatory model, where subcutaneous injection of $AANO_2$ was able to decrease NOX2 activity in macrophages from thioglycolate treated mice.

Keywords

NOX2; nitro-fatty acids; inflammation

Introduction

Arachidonic acid (AA) is a precursor of inflammatory signaling mediators by enzymatic and non-enzymatic oxidative pathways. Inflammation is characterized by the production of cytokines, AA-derived eicosanoids and reactive nitrogen (RNS) and oxygen-species (ROS), *i.e.* through the activation of inducible nitric oxide synthase (NOS2) and NADPH oxidase

[*]Address correspondence to: Andrés Trostchansky, Ph.D., Departamento de Bioquímica, Facultad de Medicina, Avda. Gral. Flores 2125, C.P. 11800, Montevideo, Uruguay; Phone: (598)-2924 9562; Fax: (598)-2924 9563; trocha@fmed.edu.uy.

(NOX), respectively [1–3]. The products of these enzymes, nitric oxide (·NO) and superoxide radical ($O_2^{\cdot-}$), are the precursors of a variety of oxidizing and nitrating agents (*e.g.* peroxynitrite) which under inflammatory conditions lead to an increase of oxidized as well as nitrated proteins and lipids [4–10]. Indeed, higher levels of ·NO and $O_2^{\cdot-}$, in addition to its dismutation product hydrogen peroxide (H_2O_2), have been implicated in many physiological and pathophysiological processes [11–14].

It has been well established that AA signaling cascades and RNS pathways are intrinsically related [15]. In fact, nitration of AA could divert the fatty acid from its normal metabolic pathway affecting prostaglandin endoperoxide H synthase activity [16–21] with unknown cell signaling consequences, *i.e.* affectation of platelet aggregation [22]. In activated macrophages, nitroarachidonic acid ($AANO_2$) exert protective anti-inflammatory actions diminishing NOS2 expression as well as secretion of pro-inflammatory cytokines [4]. We have recently reported that $AANO_2$ is an almost irreversibly inhibitor of the inducible isoform of the prostaglandin endoperoxide H synthase (PGHS-2) [23], which in addition to the down regulation of NOS2 under inflammatory stimulus should contribute to the physiological shut down of inflammatory responses in macrophages. However, less is known about the capacity of $AANO_2$ to regulate the production of ROS under pro-inflammatory conditions. Indeed, one of the open questions in the field is related to the mechanisms involved in the observed anti-inflammatory actions of $AANO_2$ at both molecular and cellular levels.

Macrophages act at the first line of defense by detecting infectious agents through membrane receptors, initiating signaling pathways leading to a wide variety of cellular responses [12,24]. One of the immediate responses involves the production of $O_2^{\cdot-}$, due to the NADPH dependent univalent reduction of oxygen to $O_2^{\cdot-}$, by the phagocytic NADPH oxidase isoform (NOX2) [11,12,24]. NOX2 is an enzyme complex comprised of a membrane–bound flavocytochrome b_{558} ($gp91^{phox}$ and $p22^{phox}$), three cytosolic subunits ($p47^{phox}$, $p40^{phox}$ and $p67^{phox}$) and GTPase Rac2 [25–29]. In resting macrophages, the NOX complex is unassembled. Upon activation, the cytosolic components associate with $gp91^{phox}$ and $p22^{phox}$ forming the active enzyme complex which at this time generates $O_2^{\cdot}$ [28,30–33]; the migration of cytosolic subunits to the membrane involves conformational changes in $p47^{phox}$ secondary to its extensive phosphorylation by protein kinase C (PKC) [34,35]. It has been suggested a strong relationship between the AA pathway and NOX2 assembly/activation [36,37]. This connection, in addition to the previously reported anti-inflammatory actions of $AANO_2$ in macrophages, leads us to propose that $AANO_2$ can modulate macrophage activation by inhibiting $O_2^{\cdot-}$ formation by NOX2. In this study, we evaluate the effects of $AANO_2$ on NOX2 activity in activated macrophages; the mechanisms involved in the observed actions were also analyzed.

Materials and Methods

Reagents

Nitroarachidonic acid was synthesized and quantitated as previously described [4]. Amplex Red, Fc-oxyBURST particles and the Alexa-Fluor 488 and Alexa-Fluor 594 conjugated anti-rabbit antibodies were from Invitrogen-Molecular Probes (Los Angeles, CA). Rabbit polyclonal anti-mouse phospho-$p40^{phox}$ and rabbit polyclonal anti-actin antibodies were from Santa Cruz Biotechnology (Heidelberg, Germany). Rabbit anti-mouse $p47^{phox}$ was from MilliPore Biotechnologies Inc. HRP conjugated anti-rabbit antibody was from Sigma Chemicals (St. Louis, MO). C57BL/6 $gp91^{phox}$–/– mice were obtained from The Jackson Laboratory (Bar Harbor, Maine) [38,39]. Animals were provided with food and water *ad libitum*. All animal studies were approved by the local authorities (CHEA, Comisión Honoraria de Experimentación Animal).

NADPH oxidase activity in macrophages

J774A.1 murine macrophage cells (ATCC, USA) were maintained by passage in Dulbecco's Modified Eagle's Medium (DMEM), supplemented with 10% heat-inactivated fetal calf serum (FCS). Rats spleen macrophages were obtained as previously described by Nakamura et al [40] with modifications. Briefly, spleen was homogenized and remaining erythrocytes lysed by hypotonic shock. Mixed cells from spleen were harvested, maintained in DMEM medium and plated in a multiwell plate. J774A.1 cells or primary macrophages were treated with AA or $AANO_2$, washed and activated at 37°C by exposing to either phorbol esters (PMA, 3 μg/ml) or opsonized Zymosan (40 mg/ml) The control conditions correspond to absence of stimulus. NOX2 activity was determined by a) $O_2^{\cdot-}$ formation by the superoxide dismutase (SOD) inhibitable-cytochrome c (cyt c) reduction assay [41], b) $O_2^{\cdot-}$-dependent luminol chemiluminescence [42,43] and c) H_2O_2 coming from $O_2^{\cdot-}$ spontaneous dismutation by Amplex Red fluorescence in the presence of HRP [44]. Opsonization of zymosan was performed by incubation with fresh human serum at 37°C for 20 min [45]. Luminol chemiluminescence and Amplex Red Fluorescence assays were followed at 37°C in a luminescence (Lumistar, BMG Labtechnologies) and a fluorescence plate reader (λ_{ex}= 515 nm, λ_{em}= 590 nm) (Fluostar, BMG Labtechnologies) respectively.

Macrophages extraction from C57BL/6 gp91^{phox}−/− mice

Superoxide production in macrophages extracted from gp91^{phox}−/− mice was evaluated after macrophages extraction from leg's bone marrow of the gp91^{phox}−/− mice and wild type (WT) mice. Mice were sacrificed at 6–12 week old and femur as well as tibia extracted in sterile PBS. Both epiphyses were removed and the bones were flushed with a syringe filled with RPMI medium to extrude bone marrow. For cell differentiation to macrophages, the obtained cells were exposed to L929-cell conditioned medium (LCCM) for 7 days as source of granulocyte/macrophage colony stimulating factor [46,47]. Finally, the obtained macrophages from the gp91^{phox}−/− and WT mice were treated with $AANO_2$ (10 μM) and $O_2^{\cdot-}$ production after PMA activation performed as previously by following cyt c reduction [41].

Flow cytometry analysis of Fc-oxyBURST oxidation

To evaluate $O_2^{\cdot-}$ released during FcγR-mediated phagocytosis, 5,7-DHCF-conjugated bovine serum albumin-IgG immune complexes (Fc-oxyBURST, Molecular Probes) was used [48]. J774A.1 macrophages were treated with methanol (vehicle), DPI (50 μM), AA (10 μM) or $AANO_2$ (10 μM) for 1hr at 37°C, washed with PBS and then incubated with Fc-oxyBURST (50 μg/ml) for an hour. Cells were harvested, washed, resuspended in dPBS, and then kept in the dark until analysis. Fluorescence due to Fc-oxyBURST oxidation was measured in a FACS Calibur (BD Biosciences) (λ_{ex}= 488 nm, λ_{em}= 530 nm) [48].

Preparation of subcellular fractions

J774A.1 macrophages were incubated with AA (10 μM) or $AANO_2$ (10 μM) by 15 min at 37°C and activated with PMA (3 μg/ml) for 15 min. The cells were harvested, washed and resuspended in subcellular fraction buffer (250 mM Sucrose, 20 mM HEPES pH 7.4, 10 mM KCl, 1.5 mM MgCl2, 1 mM EDTA, 1 mM EGTA), containing proteases inhibitors cocktail. Cells were lysed by sonication and the resultant lysate centrifuged at 1,000 g for 10 min generating the nuclear fraction (pellet) followed by a 1 hr centrifugation at 100,000 g resulting in the membrane (pellet) and cytosolic (supernatant) fractions [49]. Proteins were quantified with the Bicinchoninic acid protein assay, and fractions conserved at −80°C until used.

Western blot

Phosphorylation and translocation of cytosolic subunits were analyzed by western blot [49] using rabbit anti-mouse phospho-$p40^{phox}$ polyclonal antibody (Santa Cruz) or rabbit anti-mouse $p47^{phox}$ polyclonal antibody (Millipore Biotechnologies Inc.), respectively. To analyze the translocation of the cytosolic subunits to the membrane, both the membrane and cytosolic fractions were used to determine the presence of $p47^{phox}$. Controls performed were done using rabbit polyclonal anti-actin and rabbit polyclonal anti-$gp91^{phox}$ antibodies (Santa Cruz). HRP conjugated anti-rabbit antibody (Sigma Chemicals, USA) was used as a secondary antibody and proteins detected by chemiluminescence using SuperSignal Chemiluminescent Substrates (Pierce, USA).

Assessment of macrophages viability

Cell viability was analyzed using the MTT assay (3-(4,5-Dimethylthiazol-2-yl)-2,5-diphenyltetrazolium bromide) measuring the blue stain at 570 nm [50], and the propidium iodide (PI) assay analyzed by flow cytometry (λ_{ex}= 488 nm, λ_{em}= 617 nm, FACS Calibur, BD Biosciences) [51]. In all cases, vehicle (methanol) effects were evaluated without observing any effect on cell viability.

Macrophage phagocytosis

To study macrophage phagocytosis, we used FITC-conjugated beads [52]. Cells cultures were incubated with $AANO_2$ for 15 min at 37°C, washed and treated with the fluorescent beads at 37°C for 3hr. Cells were harvested, washed, and resuspended in dPBS buffer. Intracellular fluorescence was measured by flow cytometry (λ_{ex}= 490nm, λ_{em}= 520 nm) [52]. The effects of $AANO_2$ were compared to the phagocytic inhibitor cytochalasin A (50 μM) [53].

Confocal Microscopy assays

The differential localization of $p47^{phox}$ was analyzed by immunoflurescence confocal microscopy [54]. Macrophages were incubated for 15 min at 37°C with vehicle, AA (10 μM) or $AANO_2$ (10 μM) and activated with FITC-conjugated zymosan for 20 min at 37°C. Cells were fixed, permeabilized and blocked, and then incubated with an anti-$p47^{phox}$ antibody and an Alexa Fluor-594 goat anti-mouse IgG antibody. Samples were analyzed with a Confocal Microscopy TCS SP5 II (Leica Microsystems).

Thioglycolate induced inflammation

Male C57BL/6 mice (18–30 g) were separated in three groups, and injected subcutaneously with vehicle, $AANO_2$ or AA once a day for three days (10 μM/day). At day 0, mice were injected i.p. with thioglycolate (10%v/v) and after four days mice were sacrificed. Peritoneal macrophages were extracted by injecting cold DMEM culture medium [55] followed by evaluation of NADPH oxidase activity after cell activation with PMA. Control groups without thioglycolate for vehicle, AA and $AANO_2$ were included.

Statistical analysis

Experiments were performed at least three times on independent days. Data showed correspond to the mean ± standard deviation, unless otherwise noted. All data are given in mean and a $p < 0.05$ was considered significant. Means were compared by the Student's t test and ANOVA test.

Results

$AANO_2$ decreased superoxide radical formation by NOX2 in activated macrophages

We first evaluated the effect of $AANO_2$ on $O_2^{\cdot-}$ production in J774A.1 macrophages (Figure 1). The activation of macrophages with PMA induced an increase in $O_2^{\cdot-}$ formation as evidenced by cyt c reduction (Figure 1A), luminol luminescence (Figures 1B) and Amplex Red fluorescence (Figure 1C). Addition of SOD inhibited cyt c reduction almost completely (Figure 1A). Pre-incubation of macrophages with low micromolar levels of $AANO_2$ induced a dose-dependent inhibition of $O_2^{\cdot-}$ production (Figures 1 and 3B), with no effects observed when activated with AA treated cells (Figure 1). Accordingly, no effects on Amplex Red oxidation were observed in the presence of $AANO_2$ without PMA (supporting information, Figure 1S). Similarly, $AANO_2$ also caused an inhibition on $O_2^{\cdot-}$ detection in PMA-stimulated macrophages obtained from C57BL/6 wt animals. The specificity of $AANO_2$–dependent inhibition of $O_2^{\cdot-}$ detection was further substantiated with the use of $gp91^{phox-/-}$ mice. Indeed, we were unable to observe cyt c reduction in macrophages from $gp91^{phox-/-}$ mice upon PMA stimulation either in the absence or presence of $AANO_2$ (inset Figure 1A).

Amplex red inhibition exerted by $AANO_2$ was similar when cells activation was performed with the classic phagocytic pathway activator opsonized zymosan [45,56] or using macrophages from rat spleen (supporting information, Figure 2S) in addition to diphenyliodonium (DPI) inhibition (Figure 2 and supporting information, Figure 1S). The inhibitory effect of $AANO_2$ on NOX2 activity was time- and concentration-dependent (Figure 3A and 3B, respectively and supporting information, Figure 3S); NOX2 inhibition by the nitro-fatty acid was maximal between 15 and 30 min (Figure 3A) with an inhibitory concentration 50 (IC_{50}) of 4.1 ± 1.8 μM $AANO_2$ (Figure 3B).

NOX2 inhibition by $AANO_2$ occurs in phagosomes

Phorbol esters, *i.e.* PMA activate phosphorylation of NOX2 cytosolic components with their subsequent migration to the membrane to form the active enzyme [57]. Thus we investigated if the inhibition of NOX2 exerted by $AANO_2$ occurred in physiological mimic conditions within the phagosomes using the Fc-oxyBURST (Figure 2). After binding to membrane Fc-receptors, the Fc-oxyBURST is internalized and the H_2DCF oxidized by ROS in the phagosome to the fluorescent dichlorofluorescein (DCF) [48] which can be followed by flow cytometry (Figure 2A), a process which was inhibited by DPI (Figure 2B). When phagocytosis was activated in $AANO_2$ treated macrophages, the extent of Fc-oxyBURST oxidation was lower at both 2 and 10 μM $AANO_2$ (Figure 2B). As expected, AA was unable to decrease Fc-oxyBURST derived fluorescence (Figure 2B). Phagocytic capacity remained unaffected in the presence of $AANO_2$ when analyzed by flow cytometry using fluorescent beads (supporting information, Figure 4S).

$AANO_2$ inhibition does not affect macrophage viability

A decrease in the number of viable cells after treatment with $AANO_2$ could explain the reduction of the observed $O_2^{\cdot-}$ production. However, by using the propide iodide as well as the MTT assays [50,51], $AANO_2$ did not have any effect on macrophages viability at the experimental conditions used for NOX2 activity studies (supporting information, Figure 5S).

$AANO_2$ does not affect phosphorylation cascades while prevents active complex assembly

Phosphorylation cascades precede the assembly of the active enzyme in the membrane [33,34,36,58,59]. Phosphorylation of cytosolic components (phospho-$p40^{phox}$) increased in PMA-activated macrophages, compared to non-activated cells, at similar levels to those observed in cells incubated with $AANO_2$ (supporting information, Figure 6AS). Using an anti-phosphoserine antibody, phosphorylated proteins were inmunoprecipitated and western

blot analysis showed similar results for phopho-$p47^{phox}$ (supporting information, Figure 6BS). All together, our results demonstrate that $AANO_2$ effects were not exerted at the phosphorylation cascades necessaries for NOX2 activation. Migration of cytosolic subunits to the membrane to achieve the active form of the enzyme was tested in figure 4 by analyzing the presence of $p47^{phox}$ in both the cytosolic and membrane fraction of activated macrophages. After activation with PMA in the absence or presence of AA, $p47^{phox}$ levels were higher in the membrane fraction and lower in the cytosolic fraction compared to the non-activated cells (Figure 4). In contrast, $AANO_2$ induced a decrease in the migration of $p47^{phox}$ to the membrane as observed by both lower levels of $p47^{phox}$ in the membrane fraction and a concomitant higher concentration of the subunit in the cytosol (Figure 4). These results were confirmed by confocal microscopy studies (Figure 5): macrophages were activated in the absence or presence of $AANO_2$ or AA with FITC-conjugated zymosan (green fluorescence) and followed the migration of the cytosolic subunits using an anti-$p47^{phox}$ antibody (red fluorescence). In activated cells incubated with 10 μM of $AANO_2$, a reduced co-localization of the green and red fluorescence was observed compared to the AA condition (Figure 5).

$AANO_2$ inhibits NOX2 activity *in vivo*

Finally, the capacity of $AANO_2$ to modulate the enzyme in an inflammatory model was tested (Table 1). Thioglycolate was injected to mice that were treated with vehicle, AA or $AANO_2$ for three consecutive days (one subcutaneous injection of the compounds per day) and peritoneal macrophages were obtained at day 4. Macrophages- NOX2 activity was then analyzed with Amplex Red as previously (Table 1). Macrophages obtained from mice treated with $AANO_2$ showed a decreased formation of $O_2^{\cdot -}$ after activation with PMA compared to those from vehicle- or AA- treated animals (Table 1 and data not shown). Amplex Red fluorescence was inhibited in all experiments by the addition of DPI prior to activation with PMA (Table 1).

Discussion

We demonstrate the inhibition of phagocytic NOX2 activity by $AANO_2$ both in activated macrophages and *in vivo*. NOX2 activity was analyzed by both direct formation of $O_2^{\cdot -}$ or its dismutation product H_2O_2 using different analytical approaches (Figures 1 to 3). The involvement of NOX2 on $O_2^{\cdot -}$ production was confirmed by the inhibitory effect of SOD on cyt c reduction and the lack of $O_2^{\cdot -}$ detection in macrophages from gp91phox−/− mice (Figure 1). The $AANO_2$ effects on $O_2^{\cdot -}$ generation were observed both in a macrophage cell line (J774A.1) as well as in primary macrophages (from C57BL/6 mice and rat spleen).

We then investigated if the inhibition of NOX2 exerted by $AANO_2$ occurred under physiologically-relevant conditions within the phagosomes using the Fc-oxyBURST (Figure 2). The Fc-oxyBURST consists in a bovine serum albumin (BSA) linked to dichlorodihydrofluorescein (H_2DCF) and complexed with anti-BSA IgG antibodies, which after internalization is oxidized leading to the formation of the fluorescent dichlorofluorescein (DCF) in the phagosome [48] which can be followed by flow cytometry (Figure 2A); lower levels of Fc-oxyBURST oxidation in the presence of $AANO_2$ were observed compared to activated macrophages supporting inhibition of $O_2^{\cdot -}$ generation by the nitroalkene (Figure 2). Phagocytic capacity of macrophages when analyzed with fluorescent beads was inhibited by cytochalasin [60] but was unaffected by $AANO_2$ (supporting information, Figure 4S). One potential explanation for the observed effects on $O_2^{\cdot -}$ production could be an effect of $AANO_2$ on cell viability. Thus, we performed experiments with the propide iodide as well as the MTT assays [50,51] without observing any effect after incubation with $AANO_2$ (supporting information, Figure 5S). Overall, our results suggest

that the capacity of $AANO_2$ to decrease $O_2^{\cdot-}$ formation in the phagosome is by inhibiting NOX2 activity/assembly.

Modulation of the correct assembly of the active enzyme at the cell membrane could be a mechanism which can explain the observed $AANO_2$ enzyme inhibition. Phosphorylation cascades precede the assembly of the active enzyme in the membrane involving phosphorylation of $p47^{phox}$, and the subsequent phosphorylation of $p67^{phox}$ and $p40^{phox}$ [33,34,36,58,59]. Then, these phosphorylated proteins are triggered to migrate to the cell membrane together with Rac2 thus interacting with the membrane subunits ($gp91^{phox}$ and $p22^{phox}$) forming the active complex [24,58,61–63]. When macrophages were stimulated with PMA in the presence of $AANO_2$, the levels of phosphor-p40phox were similar to those observed in activated cells without the nitro-fatty acid (supporting information, Figure 6AS), being the role as a positive or negative regulator of phospho-$p40^{phox}$ in the activation of NOX2 controversial [58,62]. Indeed, there are reports suggesting that $p40^{phox}$ is a positive regulator of NOX2 as an adaptor protein linking the cytoplasmic complex subunits ($p40^{phox}$-$p67^{phox}$-$p47^{phox}$) to phagosomes as well as regulating p67phox translocation to the membrane [62,64]. Also, the role of p40phox could be dependent of the phosphorylation status of $p47^{phox}$ [62]. Thus we decided to study the phosphorylation of $p47^{phox}$, which is phosphorylated in a Serine residue during enzyme activation [59]. Again, no differences were observed discarding phosphorylation of cytosolic subunits as the mechanism for $AANO_2$-mediated NOX2 inhibition. Downstream phosphorylation, cytosolic subunits migrate to the membrane where they associate with $gp91^{phox}$ and $p22^{phox}$ achieving the active form of the enzyme [36,56,64]. Thus, if $AANO_2$ is able to affect the migration of the cytosolic subunits to the membrane the final result is the inhibition of NOX2 activity. This hypothesis was tested in figure 4 by analyzing the presence of $p47^{phox}$ in both the cytosolic and membrane fraction of activated macrophages. Western blot and microscopy results indicate that $AANO_2$ modulated the translocation of $p47^{phox}$ avoiding the formation of the active enzyme complex, thus inhibiting NOX2 dependent $O_2^{\cdot-}$ formation.

The effects of $AANO_2$ on NOX2 activity showed a first order decay, with a concentration exerting a reduction of 50% initial activity of 4.1 ± 1.8 μM $AANO_2$ (Figure 3A). Also, pre-incubation time had influence on the nitro-fatty acid action decreasing the inhibitory effect after 30 min suggesting a potential reversible mechanism involved in the observed action. In fact, nitroalkenes have electrophilic reactivity towards reactive nucleophilic amino acids in proteins, e.g. cysteine or histidine residues forming covalent reversible adducts responsible for many of the reported protective actions for nitro-fatty acids [65,66]. Under our experimental conditions we cannot discard that $AANO_2$ is covalently reacting with either the cytosolic or the membrane subunits, preventing the correct assembly of the active enzyme.

Thioglycolate injection into the peritoneum is a well recognized model due to its capacity to elicit an inflammatory response after 4 days, increasing the recruitment and number of macrophages [55]. Mice were treated subcutaneous once a day for four days after thioglycolate injection with vehicle, AA or $AANO_2$ and, after sacrificed macrophages were isolated, activated with PMA and analyzed for Amplex Red oxidation (Table 1). $AANO_2$ was able to decrease macrophage activation supporting a novel nitro-fatty acid anti-inflammatory role.

The data presented in this work are indicative that $AANO_2$ inhibits phagocytic NADPH oxidase in activated macrophages through a mechanism that involves the prevention of the migration of the cytosolic subunits to the membrane, affecting the correct assembly of the active form of the enzyme. The capacity of $AANO_2$ to inhibit NOX2 may generate a less active macrophage [67–69]. In a chronic inflammatory processes, where nitration of AA

may occur due to an increase of the oxidative/nitrosative stress [70–74], $AANO_2$ may inhibit key inducible enzymes (e.g. NOX2, NOS2 or PGHS-2) aiding in the resolution of inflammation. In fact, the decrease of macrophage activation in thioglycolate treated mice suggests that $AANO_2$ can exert beneficial anti-inflammatory effects when administered at pharmacological doses.

Supplementary Material

Refer to Web version on PubMed Central for supplementary material.

Acknowledgments

This work was supported by grants from Fondo Maria Viñas-ANII (FMV_2009_2913) to AT; ICGEB (Italy) to HR, Universidad de la República (CSIC, Uruguay) to HR and RR, and from the National Institutes of Health, 1R01AI095173-01 (NIH, USA) to RR. LGP was partially supported by a fellowship from Sistema Nacional de Becas-ANII.

Abbreviations

AA	arachidonic acid
$AANO_2$	nitroarachidonic acid
$O_2^{\cdot -}$	superoxide radical
NOX2	phagocytic NADPH oxidase
PMA	phorbol myristate acetate
ROS	reactive oxygen species
RNS	reactive nitrogen species
NOS2	inducible nitric oxide synthase
H_2O_2	hydrogen peroxide
cyt c	cytochrome c
SOD	superoxide dismutase
DPI	diphenyliodonium

References

1. Vachier I, Chanez P, Bonnans C, Godard P, Bousquet J, Chavis C. Endogenous anti-inflammatory mediators from arachidonate in human neutrophils. Biochem Biophys Res Commun. 2002; 290(1): 219–224. [PubMed: 11779156]
2. Cross AR, Parkinson JF, Jones OT. The superoxide-generating oxidase of leucocytes. NADPH-dependent reduction of flavin and cytochrome b in solubilized preparations. Biochem J. 1984; 223(2):337–344. [PubMed: 6497852]
3. Kakinuma K, Kaneda M, Chiba T, Ohnishi T. Electron spin resonance studies on a flavoprotein in neutrophil plasma membranes. Redox potentials of the flavin and its participation in NADPH oxidase. J Biol Chem. 1986; 261(20):9426–9432. [PubMed: 3013889]
4. Trostchansky A, Souza JM, Ferreira A, Ferrari M, Blanco F, Trujillo M, Castro D, Cerecetto H, Baker PR, O'Donnell VB, Rubbo H. Synthesis, isomer characterization, and anti-inflammatory properties of nitroarachidonate. Biochemistry. 2007; 46(15):4645–4653. [PubMed: 17373826]
5. Beckman JS, Beckman TW, Chen J, Marshall PA, Freeman BA. Apparent hydroxyl radical production by peroxynitrite: implications for endothelial injury from nitric oxide and superoxide. Proc Natl Acad Sci U S A. 1990; 87(4):1620–1624. [PubMed: 2154753]

6. Gryglewski RJ, Palmer RM, Moncada S. Superoxide anion is involved in the breakdown of endothelium-derived vascular relaxing factor. Nature. 1986; 320(6061):454–456. [PubMed: 3007998]
7. Ischiropoulos H, Zhu L, Chen J, Tsai M, Martin JC, Smith CD, Beckman JS. Peroxynitrite-mediated tyrosine nitration catalyzed by superoxide dismutase. Arch Biochem Biophys. 1992; 298(2):431–437. [PubMed: 1416974]
8. O'Donnell VB, Eiserich JP, Bloodsworth A, Chumley PH, Kirk M, Barnes S, Darley-Usmar VM, Freeman BA. Nitration of unsaturated fatty acids by nitric oxide-derived reactive species. Methods Enzymol. 1999; 301:454–470. [PubMed: 9919594]
9. Trostchansky A, Ferrer-Sueta G, Batthyany C, Botti H, Batinic-Haberle I, Radi R, Rubbo H. Peroxynitrite-mediated LDL oxidation is inhibited by manganese porphyris in the presence of uric acid. Free Rad Biol Med. 2003; 35(10):1293–1300. [PubMed: 14607528]
10. Rubbo H, Radi R, Trujillo M, Telleri R, Kalyanaraman B, Barnes S, Kirk M, Freeman BA. Nitric oxide regulation of superoxide and peroxynitrite-dependent lipid peroxidation. Formation of novel nitrogen-containing oxidized lipid derivatives. J Biol Chem. 1994; 269(42):26066–26075. [PubMed: 7929318]
11. Cathcart MK. Regulation of superoxide anion production by NADPH oxidase in monocytes/macrophages: contributions to atherosclerosis. Arterioscler Thromb Vasc Biol. 2004; 24(1):23–28. [PubMed: 14525794]
12. Alvarez MN, Trujillo M, Radi R. Peroxynitrite formation from biochemical and cellular fluxes of nitric oxide and superoxide. Methods Enzymol. 2002; 359:353–366. [PubMed: 12481586]
13. Mabley JG, Liaudet L, Pacher P, Southan GJ, Groves JT, Salzman AL, Szabo C. Part II: beneficial effects of the peroxynitrite decomposition catalyst FP15 in murine models of arthritis and colitis. Mol Med. 2002; 8(10):581–590. [PubMed: 12477968]
14. Mapp PI, Klocke R, Walsh DA, Chana JK, Stevens CR, Gallagher PJ, Blake DR. Localization of 3-nitrotyrosine to rheumatoid and normal synovium. Arthritis Rheum. 2001; 44(7):1534–1539. [PubMed: 11465704]
15. Salvemini D, Seibert K, Masferrer JL, Settle SL, Currie MG, Needleman P. Nitric Oxide Activates the Cyclooxygenase Pathway in Inflammation. Am J Ther. 1995; 2(9):616–619. [PubMed: 11854836]
16. Balazy M, Iesaki T, Park JL, Jiang H, Kaminski PM, Wolin MS. Vicinal nitrohydroxyeicosatrienoic acids: vasodilator lipids formed by reaction of nitrogen dioxide with arachidonic acid. J Pharmacol Exp Ther. 2001; 299(2):611–619. [PubMed: 11602673]
17. Di Rosa M, Ialenti A, Ianaro A, Sautebin L. Interaction between nitric oxide and cyclooxygenase pathways. Prostaglandins Leukot Essent Fatty Acids. 1996; 54(4):229–238. [PubMed: 8804119]
18. Goodwin DC, Landino LM, Marnett LJ. Effects of nitric oxide and nitric oxide-derived species on prostaglandin endoperoxide synthase and prostaglandin biosynthesis. Faseb J. 1999; 13(10):1121–1136. 1123: Goodwin DC et al. Reactions of prostaglandin en...[PMID: 10065376]Related Articles, Links. [PubMed: 10385604]
19. Blanchard-Fillion B, Souza JM, Friel T, Jiang GC, Vrana K, Sharov V, Barron L, Schoneich C, Quijano C, Alvarez B, Radi R, Przedborski S, Fernando GS, Horwitz J, Ischiropoulos H. Nitration and inactivation of tyrosine hydroxylase by peroxynitrite. J Biol Chem. 2001; 276(49):46017–46023. [PubMed: 11590168]
20. Marnett LJ. Recent developments in cyclooxygenase inhibition. Prostaglandins Other Lipid Mediat. 2002; 68–69:153–164.
21. Rouzer CA, Marnett LJ. Mechanism of free radical oxygenation of polyunsaturated fatty acids by cyclooxygenases. Chem Rev. 2003; 103(6):2239–2304. [PubMed: 12797830]
22. Salvemini D, Currie MG, Mollace V. Nitric oxide-mediated cyclooxygenase activation. A key event in the antiplatelet effects of nitrovasodilators. J Clin Invest. 1996; 97(11):2562–2568. [PubMed: 8647949]
23. Trostchansky A, Bonilla L, Thomas CP, O'Donnell VB, Marnett LJ, Radi R, Rubbo H. Nitroarachidonic acid, a novel peroxidase inhibitor of prostaglandin endoperoxide H synthases 1 and 2. J Biol Chem. 2011; 286(15):12891–12900. [PubMed: 21266582]

24. Alvarez MN, Peluffo G, Piacenza L, Radi R. Intraphagosomal Peroxynitrite as a Macrophage-derived Cytotoxin against Internalized Trypanosoma cruzi: CONSEQUENCES FOR OXIDATIVE KILLING AND ROLE OF MICROBIAL PEROXIREDOXINS IN INFECTIVITY. J Biol Chem. 2011; 286(8):6627–6640. [PubMed: 21098483]
25. Dinauer MC, Pierce EA, Bruns GA, Curnutte JT, Orkin SH. Human neutrophil cytochrome b light chain (p22-phox). Gene structure, chromosomal location, and mutations in cytochrome-negative autosomal recessive chronic granulomatous disease. J Clin Invest. 1990; 86(5):1729–1737. [PubMed: 2243141]
26. Sheppard FR, Kelher MR, Moore EE, McLaughlin NJ, Banerjee A, Silliman CC. Structural organization of the neutrophil NADPH oxidase: phosphorylation and translocation during priming and activation. J Leukoc Biol. 2005; 78(5):1025–1042. [PubMed: 16204621]
27. Vignais PV. The superoxide-generating NADPH oxidase: structural aspects and activation mechanism. Cell Mol Life Sci. 2002; 59(9):1428–1459. [PubMed: 12440767]
28. Juliet PA, Hayashi T, Iguchi A, Ignarro LJ. Concomitant production of nitric oxide and superoxide in human macrophages. Biochem Biophys Res Commun. 2003; 310(2):367–370. [PubMed: 14521919]
29. Wientjes FB, Segal AW, Hartwig JH. Immunoelectron microscopy shows a clustered distribution of NADPH oxidase components in the human neutrophil plasma membrane. J Leukoc Biol. 1997; 61(3):303–312. [PubMed: 9060453]
30. Doussiere J, Vignais PV. Diphenylene iodonium as an inhibitor of the NADPH oxidase complex of bovine neutrophils. Factors controlling the inhibitory potency of diphenylene iodonium in a cell-free system of oxidase activation. European Journal of Biochemistry. 1992; 208(1):61–71. [PubMed: 1324836]
31. Gorlach A, Brandes RP, Nguyen K, Amidi M, Dehghani F, Busse R. A gp91phox Containing NADPH Oxidase Selectively Expressed in Endothelial Cells Is a Major Source of Oxygen Radical Generation in the Arterial Wall. Circ Res. 2000; 87(1):26–32. [PubMed: 10884368]
32. Azumi H, Inoue N, Takeshita S, Rikitake Y, Kawashima S, Hayashi Y, Itoh H, Yokoyama M. Expression of NADH/NADPH oxidase p22phox in human coronary arteries. Circulation. 1999; 100(14):1494–1498. [PubMed: 10510050]
33. Ambruso DR, Cusack N, Thurman G. NADPH oxidase activity of neutrophil specific granules: requirements for cytosolic components and evidence of assembly during cell activation. Mol Genet Metab. 2004; 81(4):313–321. [PubMed: 15059619]
34. Park HS, Lee SM, Lee JH, Kim YS, Bae YS, Park JW. Phosphorylation of the leucocyte NADPH oxidase subunit p47(phox) by casein kinase 2: conformation-dependent phosphorylation and modulation of oxidase activity. Biochem J. 2001; 358(Pt 3):783–790. [PubMed: 11535139]
35. Waite KA, Wallin R, Qualliotine-Mann D, McPhail LC. Phosphatidic acid-mediated phosphorylation of the NADPH oxidase component p47-phox. Evidence that phosphatidic acid may activate a novel protein kinase. J Biol Chem. 1997; 272(24):15569–15578. [PubMed: 9182594]
36. Shiose A, Sumimoto H. Arachidonic acid and phosphorylation synergistically induce a conformational change of p47phox to activate the phagocyte NADPH oxidase. J Biol Chem. 2000; 275(18):13793–13801. [PubMed: 10788501]
37. Chang LC, Lin RH, Huang LJ, Chang CS, Kuo SC, Wang JP. Inhibition of superoxide anion generation by CHS-111 via blockade of the p21-activated kinase, protein kinase B/Akt and protein kinase C signaling pathways in rat neutrophils. Eur J Pharmacol. 2009; 615(1–3):207–217. [PubMed: 19445920]
38. Pollock JD, Williams DA, Gifford MA, Li LL, Du X, Fisherman J, Orkin SH, Doerschuk CM, Dinauer MC. Mouse model of X-linked chronic granulomatous disease, an inherited defect in phagocyte superoxide production. Nat Genet. 1995; 9(2):202–209. [PubMed: 7719350]
39. Ehrt S, Schnappinger D, Bekiranov S, Drenkow J, Shi S, Gingeras TR, Gaasterland T, Schoolnik G, Nathan C. Reprogramming of the macrophage transcriptome in response to interferon-gamma and Mycobacterium tuberculosis: signaling roles of nitric oxide synthase-2 and phagocyte oxidase. J Exp Med. 2001; 194(8):1123–1140. [PubMed: 11602641]

40. Nakamura K, Yamaji T, Crocker PR, Suzuki A, Hashimoto Y. Lymph node macrophages, but not spleen macrophages, express high levels of unmasked sialoadhesin: implication for the adhesive properties of macrophages in vivo. Glycobiology. 2002; 12(3):209–216. [PubMed: 11971865]
41. Iio M, Ono Y, Kai S, Fukumoto M. Effects of flavonoids on xanthine oxidation as well as on cytochrome c reduction by milk xanthine oxidase. J Nutr Sci Vitaminol (Tokyo). 1986; 32(6):635–642. [PubMed: 3035152]
42. Radi R, Rubbo H, Thomson L, Prodanov E. Luminol chemiluminescence using xanthine and hypoxanthine as xanthine oxidase substrates. Free Radic Biol Med. 1990; 8(2):121–126. [PubMed: 2158934]
43. Heinle H, el Dessouki J. Luminol-enhanced chemiluminescence after reaction of hydroperoxides with opsonized zymosan. J Biolumin Chemilumin. 1995; 10(2):71–76. [PubMed: 7676852]
44. Votyakova TV, Reynolds IJ. Detection of hydrogen peroxide with Amplex Red: interference by NADH and reduced glutathione auto-oxidation. Arch Biochem Biophys. 2004; 431(1):138–144. [PubMed: 15464736]
45. Wolf HM, Mannhalter JW, Salzmann HC, Gottlicher J, Ahmad R, Eibl MM. Phagocytosis of serum-opsonized zymosan down-regulates the expression of CR3 and FcRI in the membrane of human monocytes. J Immunol. 1988; 141(10):3537–3543. [PubMed: 2972775]
46. Marim FM, Silveira TN, Lima DS Jr, Zamboni DS. A method for generation of bone marrow-derived macrophages from cryopreserved mouse bone marrow cells. PLoS One. 5(12):e15263. [PubMed: 21179419]
47. Choi KD, Vodyanik M, Slukvin II. Hematopoietic differentiation and production of mature myeloid cells from human pluripotent stem cells. Nat Protoc. 6(3):296–313. [PubMed: 21372811]
48. Kaur I, Simons ER, Castro VA, Mark Ott C, Pierson DL. Changes in neutrophil functions in astronauts. Brain Behav Immun. 2004; 18(5):443–450. [PubMed: 15265537]
49. Birnie, GD. Subcellular components: preparation and fractionation. London Baltimore: Butterworth; University Park Press; 1972. p. 320
50. Twentyman PR, Luscombe M. A study of some variables in a tetrazolium dye (MTT) based assay for cell growth and chemosensitivity. Br J Cancer. 1987; 56(3):279–285. [PubMed: 3663476]
51. Nicoletti I, Migliorati G, Pagliacci MC, Grignani F, Riccardi C. A rapid and simple method for measuring thymocyte apoptosis by propidium iodide staining and flow cytometry. J Immunol Methods. 1991; 139(2):271–279. [PubMed: 1710634]
52. Shimizu K, Kobayashi M, Tahara J, Shiratori K. Cytokines and peroxisome proliferator-activated receptor gamma ligand regulate phagocytosis by pancreatic stellate cells. Gastroenterology. 2005; 128(7):2105–2118. [PubMed: 15940641]
53. Fisher E, Scharnagl H, Hoffmann MM, Kusterer K, Wittmann D, Wieland H, Gross W, Marz W. Mutations in the Apolipoprotein (apo) B-100 Receptor-binding region: Detection of apo B-100 (Arg3500->Trp) Associated with Two New Haplotypes and Evidence That apo B-100 (Glu3405->Gln) Diminishes Receptor-mediated Uptake of LDL. Clin Chem. 1999; 45(7):1026–1038. [PubMed: 10388479]
54. Li JM, Shah AM. Intracellular localization and preassembly of the NADPH oxidase complex in cultured endothelial cells. J Biol Chem. 2002; 277(22):19952–19960. [PubMed: 11893732]
55. Zhang X, Goncalves R, Mosser DM. The isolation and characterization of murine macrophages. Curr Protoc Immunol. 2008; Chapter 14(Unit 14):11.
56. Bedard K, Krause KH. The NOX family of ROS-generating NADPH oxidases: physiology and pathophysiology. Physiol Rev. 2007; 87(1):245–313. [PubMed: 17237347]
57. Cannon GJ, Swanson JA. The macrophage capacity for phagocytosis. J Cell Sci. 1992; 101(Pt 4): 907–913. [PubMed: 1527185]
58. Lopes LR, Dagher MC, Gutierrez A, Young B, Bouin AP, Fuchs A, Babior BM. Phosphorylated p40PHOX as a negative regulator of NADPH oxidase. Biochemistry. 2004; 43(12):3723–3730. [PubMed: 15035643]
59. Chen Q, Powell DW, Rane MJ, Singh S, Butt W, Klein JB, McLeish KR. Akt phosphorylates p47phox and mediates respiratory burst activity in human neutrophils. J Immunol. 2003; 170(10): 5302–5308. [PubMed: 12734380]

60. Hoffmann EK, Rasmussen L, Zeuthen E. Cytochalasin B: aspects of phagocytosis in nutrient uptake in Tetrahymena. J Cell Sci. 1974; 15(2):403–406. [PubMed: 4368556]
61. Pagano PJ, Clark JK, Cifuentes-Pagano ME, Clark SM, Callis GM, Quinn MT. Localization of a constitutively active, phagocyte-like NADPH oxidase in rabbit aortic adventitia: enhancement by angiotensin II. Proc Natl Acad Sci U S A. 1997; 94(26):14483–14488. [PubMed: 9405639]
62. Ueyama T, Nakakita J, Nakamura T, Kobayashi T, Kobayashi T, Son J, Sakuma M, Sakaguchi H, Leto TL, Saito N. Cooperation of p40(phox) with p47(phox) for Nox2-based NADPH oxidase activation during Fcgamma receptor (FcgammaR)-mediated phagocytosis: mechanism for acquisition of p40(phox) phosphatidylinositol 3-phosphate (PI(3)P) binding. J Biol Chem. 2011; 286(47):40693–40705. [PubMed: 21956105]
63. McLaughlin NJ, Banerjee A, Khan SY, Lieber JL, Kelher MR, Gamboni-Robertson F, Sheppard FR, Moore EE, Mierau GW, Elzi DJ, Silliman CC. Platelet-activating factor-mediated endosome formation causes membrane translocation of p67phox and p40phox that requires recruitment and activation of p38 MAPK, Rab5a, and phosphatidylinositol 3-kinase in human neutrophils. J Immunol. 2008; 180(12):8192–8203. [PubMed: 18523285]
64. Ueyama T, Tatsuno T, Kawasaki T, Tsujibe S, Shirai Y, Sumimoto H, Leto TL, Saito N. A regulated adaptor function of p40phox: distinct p67phox membrane targeting by p40phox and by p47phox. Mol Biol Cell. 2007; 18(2):441–454. [PubMed: 17122360]
65. Batthyany C, Schopfer FJ, Baker PR, Duran R, Baker LM, Huang Y, Cervenansky C, Branchaud BP, Freeman BA. Reversible Post-translational Modification of Proteins by Nitrated Fatty Acids in Vivo. J Biol Chem. 2006; 281(29):20450–20463. [PubMed: 16682416]
66. Schopfer FJ, Batthyany C, Baker PR, Bonacci G, Cole MP, Rudolph V, Groeger AL, Rudolph TK, Nadtochiy S, Brookes PS, Freeman BA. Detection and quantification of protein adduction by electrophilic fatty acids: mitochondrial generation of fatty acid nitroalkene derivatives. Free Radic Biol Med. 2009; 46(9):1250–1259. [PubMed: 19353781]
67. Babior BM. NADPH Oxidase: An Update. Blood. 1999; 93(5):1464–1476. [PubMed: 10029572]
68. Pizzolla A, Hultqvist M, Nilson B, Grimm MJ, Eneljung T, Jonsson IM, Verdrengh M, Kelkka T, Gjertsson I, Segal BH, Holmdahl R. Reactive Oxygen Species Produced by the NADPH Oxidase 2 Complex in Monocytes Protect Mice from Bacterial Infections. J Immunol. 2012
69. Sareila O, Kelkka T, Pizzolla A, Hultqvist M, Holmdahl R. NOX2 complex-derived ROS as immune regulators. Antioxid Redox Signal. 2011; 15(8):2197–2208. [PubMed: 20919938]
70. O'Donnell VB, Eiserich JP, Chumley PH, Jablonsky MJ, Krishna NR, Kirk M, Barnes S, Darley-Usmar VM, Freeman BA. Nitration of unsaturated fatty acids by nitric oxide-derived reactive nitrogen species peroxynitrite, nitrous acid, nitrogen dioxide, and nitronium ion. Chem Res Toxicol. 1999; 12(1):83–92. [PubMed: 9894022]
71. Rubbo H, Radi R. Protein and lipid nitration: role in redox signaling and injury. Biochim Biophys Acta. 2008; 1780(11):1318–1324. [PubMed: 18395525]
72. Schopfer FJ, Lin Y, Baker PR, Cui T, Garcia-Barrio M, Zhang J, Chen K, Chen YE, Freeman BA. Nitrolinoleic acid: an endogenous peroxisome proliferator-activated receptor gamma ligand. Proc Natl Acad Sci U S A. 2005; 102(7):2340–2345. [PubMed: 15701701]
73. Trostchansky A, Rubbo H. Lipid nitration and formation of lipid-protein adducts: biological insights. Amino Acids. 2007; 32(4):517–522. [PubMed: 17058116]
74. Trostchansky A, Rubbo H. Nitrated fatty acids: mechanisms of formation, chemical characterization, and biological properties. Free Radic Biol Med. 2008; 44(11):1887–1896. [PubMed: 18395528]

- Nitro-arachidonic acid exerts protective activities during macrophage activation.
- We propose that Nitro-arachidonic acid modulates phagocytic NADPH oxidase activity/assembly.
- Nitro-arachidonic acid prevents the migration of cytosolic subunits to the membrane.
- Protective effects were also observed in an *in vivo* inflammatory model.

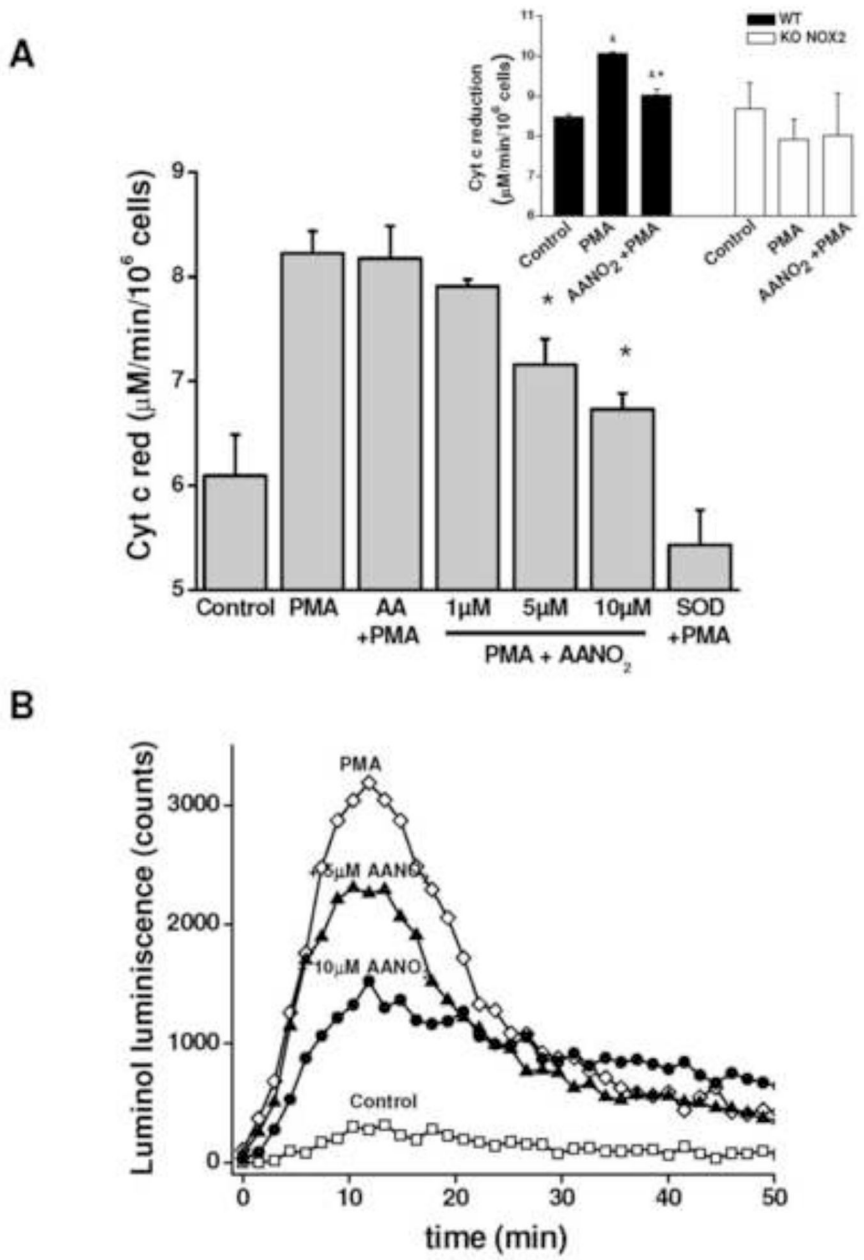

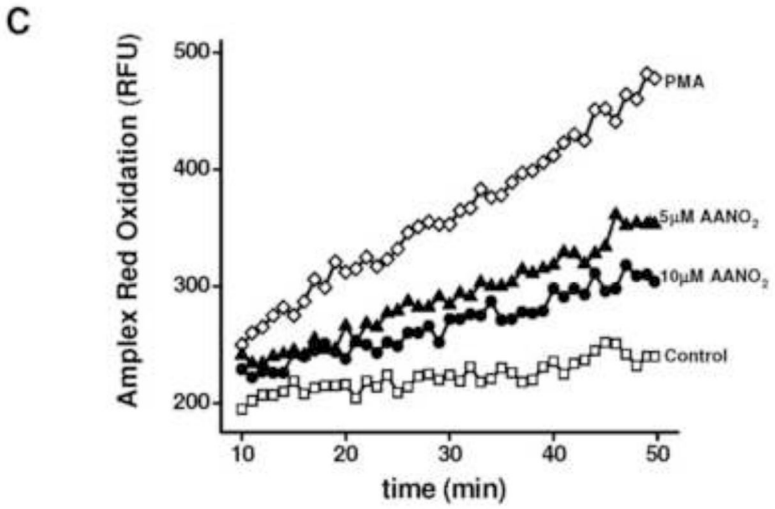

Figure 1. $AANO_2$ inhibits $O_2^{\cdot-}$ production in activated macrophages

The production of $O_2^{\cdot-}$ was analyzed in macrophages by cytochrome c reduction (**A**), Luminol chemiluminescence (**B**), and Amplex Red fluorescence in the presence of HRP (**C**). (**A**) J774A.1 macrophages (2×10^5 cells) were treated with $AANO_2$ (1, 5 and 10 μM) or AA (10 μM) for 15 minutes in dPBS buffer at 37°C, washed and activated for an additional hour with PMA (3 μg/ml) in the presence of 20 μM cyt c. The supernatant was collected and the levels of reduced cyt c due to $O_2^{\cdot-}$ were measured at 550 nm (ε= 21 mM^{-1}. cm^{-1}) [41]. A control with SOD (600 U/ml) was included. Results shown correspond to the mean ± SD, *n*=3. ** indicates statistical differences compared to the PMA condition, $p < 0.05$.* Inset: Macrophages from bone marrow of wt and $gp91^{phox-/-}$ mice were treated with 10 μM $AANO_2$ for 15 minutes in dPBS buffer at 37°C, washed and activated for an additional hour with PMA (3 μg/ml) in the presence of 20 μM cyt c. Superoxide production was evaluated by the cyt c reduction assay. ** indicates statistical differences compared to the control condition, $p < 0.05$; & indicates statistical differences compared to the PMA condition, $p < 0.05$* (**B**) J774A.1 macrophages (2×10^5 cells) were treated with $AANO_2$ (5 and 10 μM, -▲- and -●- respectively) and PMA (-◇-) as in (A). Luminol (100 μM) was added and the formation of $O_2^{\cdot-}$ was analyzed following oxidized luminol luminescence for 1hr. A control condition without PMA was also included (-□-). (**C**) Macrophages (-□-) treated with 5 μM (-▲-) and 10 μM (-●-) $AANO_2$ in dPBS buffer at 37°C, were activated with PMA (3 μg/ml, -◇-). In this case, the formation of $O_2^{\cdot-}$ derived-H_2O_2 was evaluated by following the fluorescence of Amplex Red (50 μM) with 4 μg/ml HRP (λ_{ex}= 515 nm, λ_{em}= 590 nm) in a fluorescence plate reader. Data shown in figures (B) and (C) are representative of at least four independent experiments.

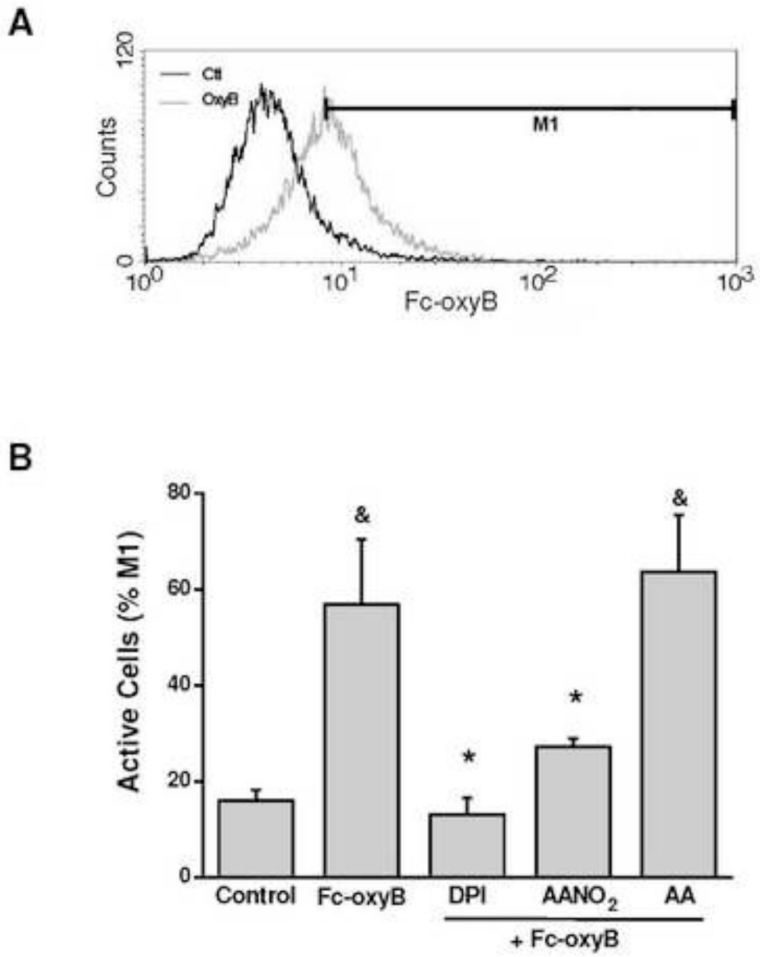

Figure 2. Flow cytometry analysis of NOX2 inhibition by $AANO_2$

J774-A1 macrophages (2×10^6 cells) were treated with $AANO_2$ (0–10 μM) or DPI (50 μM), a nonspecific NOX inhibitor. Cells were washed and treated with Fc-oxyBURST (Fc-oxyB, 50 μg/ml) for 1h, and fluorescence of DCF determined by flow cytometry. Representative histograms are shown in A and quantitative analysis of the obtained histograms was done (B). M1 region corresponds to the cell population which exhibits high fluorescence due to H_2DCF oxidation to DCF by ROS. Results shown correspond to the mean ± SD, n=3. *& indicate statistical differences compared to the control condition, $p < 0.05$; * indicate statistical differences compared to the non-inhibitor condition, $p < 00.05$.*

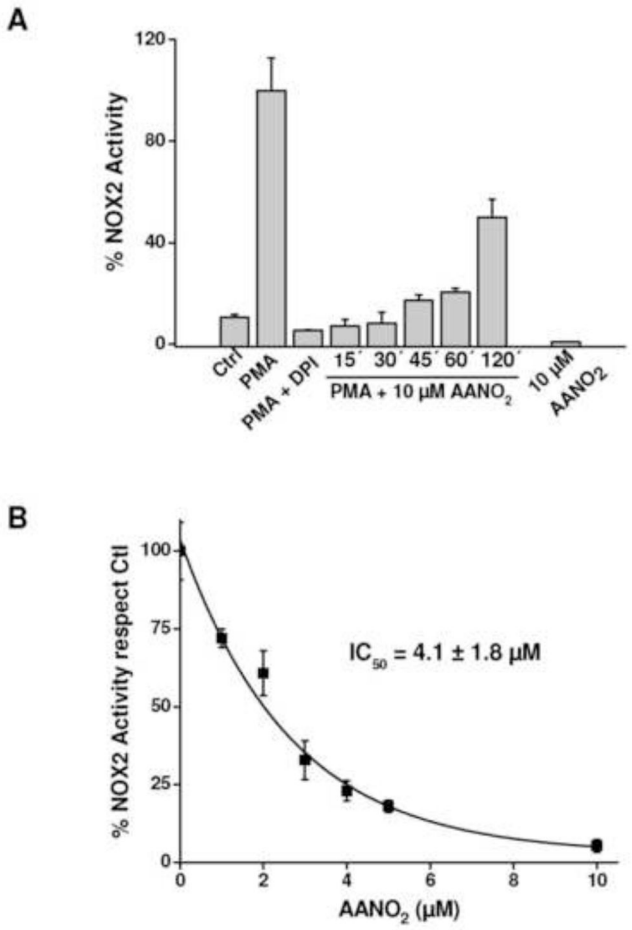

Figure 3. Time- and concentration-dependent inhibition of NOX2 by $AANO_2$

(**A**) J774A.1 macrophages (2×10^5 cells) were activated with PMA (3 μg/ml) after incubation with 10 μM $AANO_2$ for different pre-incubation times (15–120 min). NOX2 activity was analyzed by luminol chemiluminiscence as before. Controls without activation, DPI addition (50 μM), and incubation with $AANO_2$ in the absence of PMA were included. (**B**) J774A.1 macrophages (2×10^5 cells) were incubated with increasing doses of $AANO_2$ (0–10 μM) for 15 minutes and then activated with PMA (3 μg/ml); NOX2 activity was analyzed by Amplex Red fluorescence as previously. In both (A) and (B), results shown correspond to the mean ± SD, n=3 representative of at least 4 independent experiments.

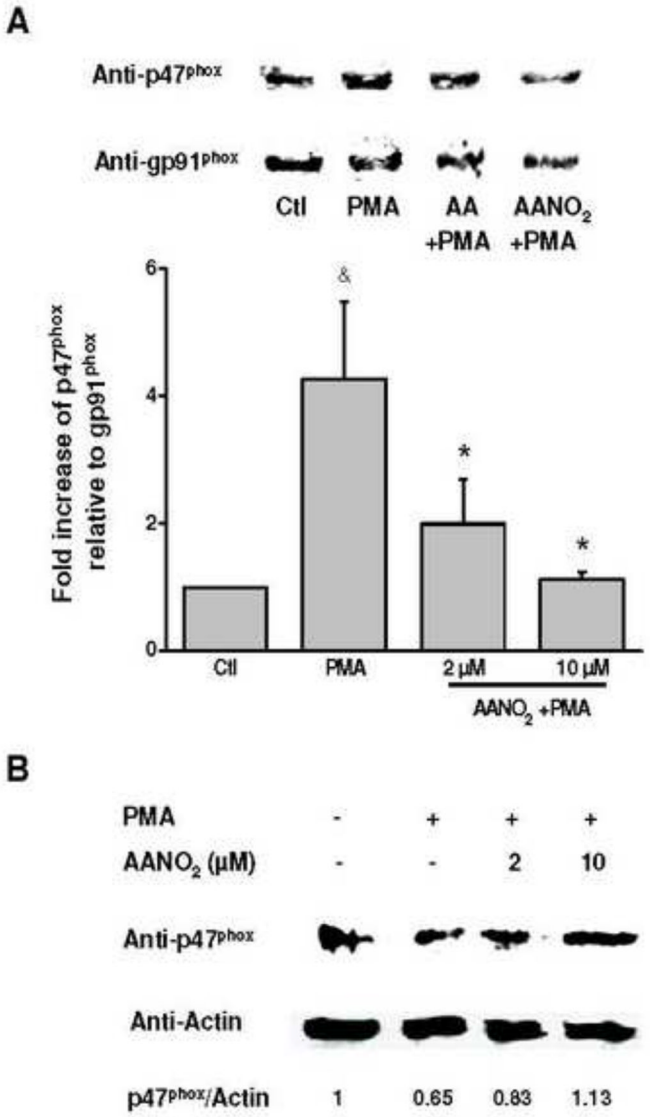

Figure 4. Translocation of cytosolic p47^{phox} to the membrane is prevented by $AANO_2$

The effects of $AANO_2$ on the migration of cytosolic subunits to the membrane were evaluated in activated macrophages. Macrophages (3×10^6 cells) were treated with $AANO_2$ (2 and 10 μM) for 15 minutes, washed and PMA-activated as previously. Cells were harvested and membrane (**A**) as well cytosolic (**B**) fractions were obtained by differential centrifugation. The presence of p47^{phox} was determined by western blot. In parallel, the levels of gp91^{phox} (**A**) as well as actin (**B**) were determined as reporters of membrane and cytosolic constitutive proteins, respectively. In (**A**) the bars represent the relative presence of p47^{phox} respect to gp91^{phox}, and results shown correspond to the mean ± SD, n=3. *& indicates statistical difference compared to the control condition, $p < 0.05$; * indicates statistical difference compared to the PMA-activated condition, $p < 0.05$.*

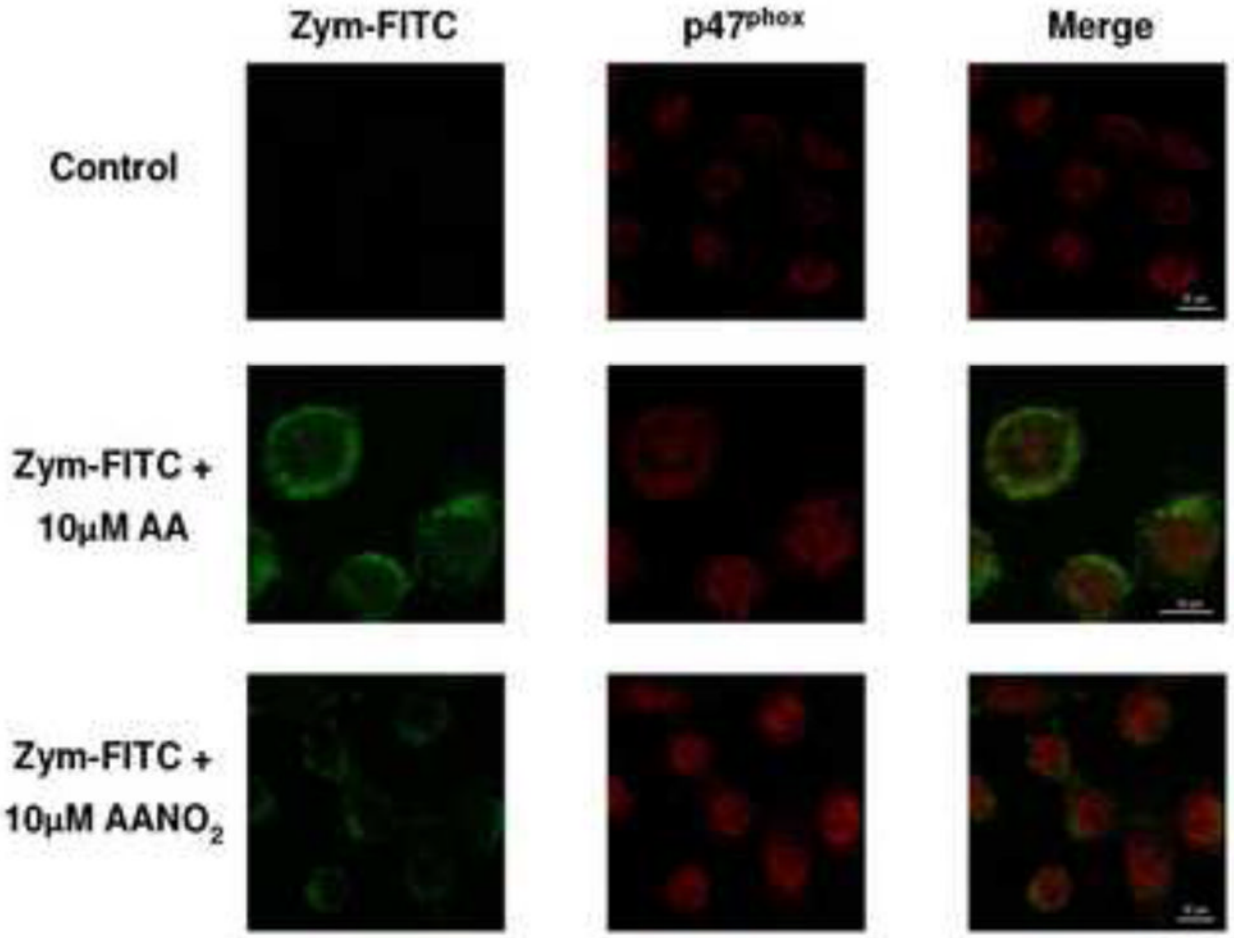

Figure 5. $p47^{phox}$ does not migrate to the membrane in the presence of $AANO_2$

J774A.1 macrophages were incubated with AA (10 μM) or $AANO_2$ (10 μM) as before. Cells were washed and activated with FITC-conjugated zymosan at 37°C. Then, permeated cells were incubated with rabbit anti-mouse $p47^{phox}$ antibody followed by the addition of a secondary Alexa Fluor 594 goat anti-mouse IgG antibody. The intracellular localization of the FITC-zymosan (green fluorescence) and $p47^{phox}$ (red fluorescence) was observed by confocal microscopy.

Table 1

Inhibition of NOX2 by $AANO_2$ in an *in vivo* model of inflammation

Mice were treated with i/p thioglycolate and subcutaneous injected with $AANO_2$ and peritoneal macrophages were obtained at day 4 as explained in the experimental section. The formation of $O_2^{\cdot -}$ derived-H_2O_2 in PMA activated-macrophages was evaluated by Amplex Red as previously. DPI addition was performed to isolated macrophages 30 min before PMA addition. Data shown correspond to the mean ± SD, n=4 representative of at least 3 independent experiments.

Condition	NOX2 activity (%)
Vehicle treated mice	25.9 ± 12.8
$AANO_2$ treated mice	5.7 ± 3.9[a]
Vehicle mice + PMA	100 ± 22.6
$AANO_2$ mice + PMA	21.7 ± 10.3[b]
Vehicle mice + PMA + DPI	27.1 ± 6.4[b]
$AANO_2$ mice + PMA + DPI	5.9 ± 1.9[b]

[a] indicates statistical difference compared to the Vehicle treated mice, $p < 0.05$.

[b] indicates statistical difference compared to the Vehicle mice +PMA, $p < 0.05$.